Neoplasma 2023; 70(4): 514–525

doi:10.4149/neo_2023_230404N185

Novel model of triple-negative breast cancer produces viable circulating tumor cells and rapid lung metastasis for functional testing *in vivo*

Jana PLAVA[1,2,*], Lenka TRNKOVA[1], Peter MAKOVICKY[1,3], Michal MEGO[4,5], Svetlana MIKLIKOVA[1,#], Lucia KUCEROVA[1,5,#]

[1]*Biomedical Research Center of the Slovak Academy of Sciences, Bratislava, Slovakia;* [2]*Institute of Medical Biology, Genetics and Clinical Genetics, Faculty of Medicine, Comenius University in Bratislava, Bratislava, Slovakia;* [3]*Department of Histology and Embryology, Faculty of Medicine, University of Ostrava, Ostrava, Czech Republic;* [4]*2nd Department of Oncology, Faculty of Medicine, Comenius University, National Cancer Institute, Bratislava, Slovakia;* [5]*Translational Research Unit, 2nd Department of Oncology, Comenius University, Faculty of Medicine, National Cancer Institute, Bratislava, Slovakia*

**Correspondence: jana.plava@savba.sk*
[#]Contributed equally to this work.

Received April 4, 2023 / Accepted July 19, 2023

Breast cancer metastases are the main reason for women´s highest cancer mortality. Even though tumor cell dissemination via circulating tumor cells (CTC) released from the primary site is a very ineffective process, distant metastases appear in 46% of triple-negative breast cancer (TNBC) patients corresponding to the disease aggressiveness. Laboratory models for functional testing which mimic the spread of metastatic cells are needed for efficient investigation of the underlying mechanisms and therapeutic intervention. Here, we describe novel isogenic variants LMC3 and CTC3 of human TNBC cell line MDA-MB-231 that were derived by repeated injection of tumor cells into the tail vein of immunodeficient mice and subsequent selection of metastatic cells from lung metastases. These variants have increased migration potential, altered expression profiles, and elevated tumorigenic potential. Moreover, cell line CTC3 readily produces metastases in the lungs and bone marrow and detectable viable circulating tumor cells in the blood. This model enables rapid and cost-efficient strategies for biomarker exploration and novel intervention approaches to limit the CTC presence in the blood and hence tumor dissemination.

Key words: breast cancer; circulating tumor cells; lung metastasis; animal model; isogenic cell line variants

In women, breast cancer is the most commonly diagnosed cancer and the leading cause of cancer death. In numbers, breast cancer accounts for 1 in 4 cancer cases and 1 in 6 cancer deaths, ranking first in incidence in the vast majority of countries (159 of 185 countries) and for mortality in 110 countries [1]. While the primary tumors are quite well manageable, metastatic disease is the main problem leading to the patient's death. The most common sites of distant metastasis in breast cancer remain the lungs and bone marrow, followed by the liver and brain [2]. Identification of predictive and prognostic biomarkers as well as a therapeutic intervention to limit metastatic spread at an early stage would have a major impact on the survival of breast cancer patients.

The metastatic process is a complicated cascade mediated by the complex crosstalk between cancer cells and their supporting stroma, mostly known as the tumor microenvironment [3]. This multi-step process requires the dissemination of cancer cells from the primary tumor, intravasation into the vascular system, transition to a distant site, extravasation from the vasculature into the secondary site, and colonization in the secondary organ [4]. The entire process cannot be fully mimicked under the *in vitro* conditions, specifically the key attributes of circulating tumor cells (CTC) capable to survive the whole process. Hence, the research on breast cancer metastasis has benefited greatly from the use of mouse models of experimental metastasis and CTC [5].

In recent years, numerous breast cancer cell lines have been injected intravenously into the tail vein [6], carotid artery [7], iliac artery [8], or even intracardially [8] into the immunodeficient mice, leading to different metastatic outcomes. Lately, the method of orthotopic injection into the mammary fat pad has been used to produce *in vivo* metastatic models. PDX (Patient-Derived Xenografts) models, in which cultured or even never-cultured patient biopsies are engrafted directly into mice, have been found to capture molecular features and heterogeneity of origi-

nating patients' tumors and serve as a resource of minimally manipulated human tumor cells [10, 11].

These approaches have different benefits and limitations for metastatic cancer research. Injection of the cancer cells directly into the bloodstream leads to a shorter duration of the experiment, and it is accepted as a valuable model mimicking the metastatic process from the step of intravasation of cancer cells. Orthotopic injection remains an ideal model to study the metastatic process from the first step, which requires cancer cell dissemination [12]. However, the generation of such models requires months to create metastatic sites and depends on the availability of biopsies from suitable donors. The main drawback of all these models is the reliance on immune-compromised mice, which leads to the limited impact of the immune system on metastasis even though we know that tumor stroma greatly affects the whole process. Despite these limitations, experimental mouse models of metastasis have provided an irreplaceable approach to interrogating all aspects of the metastatic cascade.

In our *in vivo* metastatic cancer cell line derivation, we injected triple-negative breast cancer (TNBC) cell line MDA-MB-231 together with mesenchymal stromal cells (MSC), which are greatly represented in the tumor stroma of breast cancer patients, into the immunodeficient mice. According to Rowan and colleagues [13] and also our previous work [14], MSC can promote the migration of cancer cells and increase their metastatic potential. Using MSC in our experimental design gives us higher chances to increase the number of cancer cells with the ability to metastasize into the lung. The lungs are among the first sites of metastasis in almost one-quarter of metastatic breast cancer patients [2].

Here, we established novel isogenic variants of aggressive human TNBC cell line MDA-MB-231 initiated by subcutaneous injection of tumor cells in combination with stromal cells followed by repeated intravenous injection. Hence, the tumor cells initially completed the metastatic cascade *in vivo* mimicking the clinical situation. The established variants were tested for basic functional and molecular characteristics. They represent valuable models for the investigation of approaches that intervene with the dissemination of cells from the primary tumor, decrease/eliminate CTC in the blood, and metastatic burden.

Materials and methods

Cell culture. Human mammary gland adenocarcinoma cell lines MDA-MB-231 (ATCC® HTB-26™) and JIMT-1 (DSMZ no.: ACC 589) were transduced with IncuCyte® NucLight Lentivirus Reagents (Essen BioScience, Ann Arbor, MI, USA) to express a nuclear red fluorescent protein mKate2 and carry puromycin resistance (further as NLR-MDA and NLR-JIMT). More aggressive variants of these cell lines were derived using immunodeficient SCID/Beige mice (see below). Cells were cultured in high-glucose (4.5 g/l) Dulbecco's modified Eagle medium (DMEM, PAA Laboratories GmbH, Pasching, Austria) supplemented with 10% fetal bovine serum (FBS, Biochrom AG, Berlin, Germany), 2 mM glutamine (PAA Laboratories GmbH), 10,000 IU/ml penicillin (Biotica, Part. Lupca, Slovakia), 5 µg/ml streptomycin (PAA Laboratories GmbH) and 2.5 µg/ml amphotericin B (Sigma-Aldrich, Taufkirchen, Germany).

Mesenchymal stromal cells (MSC) were isolated and characterized according to the protocol published in Kucerova et al. [15] and were maintained in low-glucose (1 g/l) DMEM supplemented with the same concentration of serum and antibiotics. All cells were cultured at 37 °C in a humidified atmosphere and 5% CO_2.

Adipose tissue donor provided informed consent and all procedures were approved by the Ethics Committee of the Ruzinov University Hospital and the National Cancer Institute (TRUSK-003), Bratislava, Slovakia.

Derivation of metastatic cancer cells *in vivo*. All animals in this study were used in accordance with institutional guidelines and approved protocols. The mixture of 1×10^6 NLR-MDA and 5×10^5 MSC re-suspended in 100 µl of serum-free DMEM diluted 1:1 with ECM gel (Sigma-Aldrich) were bilaterally subcutaneously injected onto the back of 6-weeks old SCID/Beige mice (n=2; Charles River, Germany). The animals were sacrificed according to the ethical guidelines when the tumor volume exceeded 1 cm^3. Lungs were dissociated into the cell suspension using a human Tumor Dissociation Kit (Miltenyi Biotec, Bergisch Gladbach, Germany) according to the manufacturer's protocol. Isolated cells were cultured in the complete tumor cell media supplemented with 0.5 µg/ml puromycin (InvivoGen, San Diego, CA, USA) to select metastatic and expand viable NLR-MDA cells. These cells are further mentioned as LMC1 (Lung Metastatic Cells 1). Afterward, two million of metastatic LMC1 cells were intravenously injected in 100 µl of PBS into the tail vein of 6-weeks old SCID/Beige mice. Mice were sacrificed when they exhibited weight loss, ruffled fur, breathing difficulties, or other signs of distress. The lungs were homogenized and isolated cells selected on puromycin were marked as LMC2. Two million of these cells were intravenously injected into the tail vein of 6-weeks old SCID/Beige mice. The lung was homogenized and isolated cancer cells were named LMC3. Blood samples were lysed for the possible presence of CTC, further mentioned as CTC3. Briefly, blood samples were collected into the EDTA-coated blood collection tubes, lysis buffer (0.8% NH_4Cl, 0.1mM EDTA, 0.1% $KHCO_3$, pH 7.4–7.6) was added to the samples in the ratio 9:1 (9 parts lysis buffer:1 part blood), samples were centrifuged 5 min at 150×g, washed with PBS, centrifuged again and pellets were seeded onto culture plates. Afterward, only 1×10^5 of LMC3 or CTC3 were intravenously injected in 100 µl of PBS into the tail veins of SCID/Beige mice. Metastatic cells isolated from the lungs were named LMC4.

To monitor the tumorigenicity of derived cell lines, NLR-MDA (n=3), LMC3 (n=3), and CTC3 (n=3) were bilaterally subcutaneously injected (1×10^6 cells in 100 µl serum-free DMEM diluted 1:1 with ECM gel) into the 6-weeks old SCID/Beige mice. Animals were regularly inspected for tumor growth and the tumor volume was calculated according to the formula: volume = length × width^2/2. In accordance with the ethical guidelines, animals were sacrificed when the tumors exceeded 1 cm^3.

To analyze the metastatic potential of these cells, NLR-MDA (n=3), LMC3 (n=3), and CTC3 (n=6) were intravenously injected into the tail veins of 8-week-old female NSG mice (2.5×10^5 cells in 100 µl PBS). Mice were sacrificed after 3 weeks – blood (lysed) and bone marrow from the femur were processed and seeded on the Petri dishes for the detection of fluorescent red cancer cells; lung, liver, and brain were fixed in formalin for subsequent histological and immunohistochemical analyses.

All *in vivo* experiments were performed in an authorized animal facility under license No. SK UCH 02017 and approved by the institutional ethics committee and by the national competent authority of the State Veterinary and Food Administration of the Slovak Republic (Registration Number Ro:1976/17-221) in compliance with Directive 2010/63/EU of the European Parliament and the European Council and Regulation 377/2012 for the protection of animals used for scientific purposes.

Morphology, proliferation, and migration. Basic morphology and red fluorescence of cells were captured using IncuCyte ZOOM™ kinetic imaging system (Essen BioScience). After short-term cultivation, immunocytochemistry was used to stain the cytoskeleton. Cells were washed with PBS and fixed with 4% PFA for 20 min. After incubation with an anti-F-actin antibody (Alexa Fluor® 488-Phalloidin, Molecular Probes, OR, USA), cells were mounted with Fluoromount-G® (SouthernBiotech, Birmingham, AL, USA). Stained cells were analyzed with Zeiss Axiolab 5 fluorescent microscope (Zeiss, Germany). For proliferation monitoring, 1,500 cells/well were seeded on the 96-well plate and were monitored every 2 h for 5 days until they reached confluence. The tumor cell number was evaluated using Phase Object Confluence Mask (IncuCyte ZOOM kinetic imaging system). Cell migration was evaluated in the 96-well Image Lock plates, where 35×10^3 cells/well were seeded and analyzed by IncuCyte® Scratch Wound Cell Migration and Invasion System and documented by the IncuCyte ZOOM™ kinetic imaging system.

Drug sensitivity. To evaluate the chemosensitivity to 5-fluorouracil (5-FU), cyclophosphamide (CPX), cisplatin (CisPt), doxorubicin (DOX), and paclitaxel (PTX), cells were seeded in the 96-well plates in triplicates (1.5×10^3 cells/well) and let attached overnight. Next day, the cells were exposed to 5-FU (1 µg/ml; Sigma-Aldrich), CPX (50 µg/ml, Selleck Chemicals, Houston, USA), CisPt (0.5 µg/ml, Hospira UK Ltd, Warwickshire, UK), DOX (25 ng/ml, Sigma-Aldrich), or PTX (4 ng/ml; Selleck Chemicals) and cultured for 5 days. Cell viability after exposure was measured using CellTiter-Glo® Luminescent Cell Viability Assay (Promega Corporation, Madison, WI, USA) according to the manufacturer's protocol and measured on GloMax® Discover System (Promega Corporation). The luminescence of unexposed cells was used as a reference. Values were expressed as the means of replicates ± SD. Experiments were repeated 3× and representative results are shown.

Gene expression analysis. RNA from 1×10^6 NLR-MDA, LMC3, and CTC3 were isolated using RNeasy® Mini Kit and transcribed to cDNA by RT^2 First Strand Kit (both Qiagen, Hilden, Germany). To analyze the expression of 84 metastasis-related genes in LMC3 cells, The Human Tumor Metastasis RT^2 Profiler™ PCR Array (PAHS-028ZD, Qiagen) was used. The Human Extracellular Matrix and Adhesion Molecules RT^2 Profiler™ PCR Array (PAHS-013ZD, Qiagen) was used to identify differences between parental and CTC3 cells in 84 different genes. Quantitative real-time PCR was performed using SYBR® Green qPCR Mastermix (Qiagen) and Bio-Rad CFX96™ Touch Real-Time PCR Detection system (Bio-Rad Laboratories Ltd). The CT cut-off was set at 35, and targets expressed at very low levels or undetected in the control group (= NLR-MDA) were excluded from the relative expression calculations.

Histology and immunohistochemistry. The material was fixed in a 10% neutral buffered formalin solution (Sigma-Aldrich) for 24 h, processed, and embedded into paraffin blocks. All the blocks were cut on a Hyrax M40 rotary microtome (Zeiss, Germany), and tissue sections were placed on specialized Star Frost® glass slides (Waldemar Knittel, Germany). The first series of sections were stained with standard hematoxylin-eosin staining (Bamed, Czech Republic). The next series of cuts were processed by special immunohistochemical techniques using the following antibodies: Monoclonal Mouse Anti-Human Cytokeratin 7 Clone OV-TL 12/30 Ready-to-Use Link (Dako Omnis, Denmark), Monoclonal Mouse Anti-Human Cytokeratin 20 Clone KS 208 Ready-to-Use Link (Dako Omnis, Denmark), Monoclonal Mouse Anti-Human Ki-67 Antigen Clone MIB-1 Ready-to-Use Link (Dako Omnis, Denmark). Before immunostaining, heat-induced antigen retrieval was performed by 20 min treatment in a PT Link (Dako Omnis, Denmark), using pH 9.0 buffer (EnVision Flex Target Retrieval Solution, High pH, Dako Omnis, Denmark). The slices were allowed to cool and incubated for 30 min at room temperature with antibodies. Tissue sections were washed with conventional wash buffer (EnVision Flex Wash Buffer, Dako Omnis, Denmark). For visualization, an LSAB2 System-HRP (Dako Omnis, Denmark) has been applied according to instructions. The reaction was visualized with EnVision Flex DAB+chromogen (Dako Omnis, Denmark). In the end, sections were stained with Mayer hematoxylin (Bamed, Czech Republic). The samples were evaluated and described using a microscope (Axiovert 200, Zeiss, Germany).

Statistical analysis. GraphPad Prism 6.0.1. software (La Jolla, CA, USA) was used for statistical analysis. The normality of data distribution was assessed by the Shapiro-Wilk test. According to the Gaussian distribution of data, one-way analysis of variance (ANOVA) with Dunnett T3 multiple comparison test or non-parametric Kruskal-Wallis with Dunn's multiple comparison test was used to compare differences in measured variables between derived and control groups. The p-values <0.05 were considered to be statistically significant.

Results

Derivation of novel isogenic cell line variants LMC3 and CTC3 of MDA-MB-213. To derive novel LMC3 and CTC3 models, we bilaterally subcutaneously injected NLR-MDA or NLR-JIMT1 together with MSC into the 6-week-old female SCID/Beige mice. When the tumors exceeded 1 cm^3, mice were sacrificed and their lungs were dissociated to isolate fluorescently labeled tumor cells that were capable to form lung metastasis spontaneously (Figure 1A). Cell suspensions were seeded as standard adherent cultures. We were not able to isolate any viable cancer cells from the lungs of the mice injected with the mixture of NLR-JIMT and MSC, even though we tried repeatedly.

No visible (macroscopic) metastases were observed in the mice injected with NLR-MDA mixed with MSC, however viable adherent red fluorescent cells were detected. Cells were subsequently treated by puromycin to select for tumor cell population and these cells were named LMC1. Two millions of these cells were injected into the tail veins of 6-week-old female mice in the second round of *in vivo* selection. Mice were sacrificed after one month; lungs were processed and cancer cells expanded as above and named LMC2. The same procedure was used in the third round of selection and the LMC3 line was established. In one of the animals from this cohort, we observed macroscopically metastatic spread all over the lungs and kidneys during necropsy, plus the abdomen was filled with an ascitic fluid containing tumor cells. Cells obtained from the lysed blood adhered and we detected propagating viable red flores-cent tumor cells. We named these cells CTC3 (Figure 1B). We concluded, that repeated *in vivo* passaging resulted in the selection of highly aggressive variants of tumor cells capable of very efficient lung engraftment associated with CTC presence in the mouse blood and proceeded to downstream analysis. The aggressiveness of the cells was confirmed in the next round of testing when even a 10-fold lower cell dose resulted in sudden animal death within 4–5 weeks (n=6/group). Post-mortem analysis of the material by PCR confirmed the presence of human sequences in pleural effusion (data not shown). Of note, the derivation of cell line variants from animals was performed in parallel, however, no significant differences were observed among

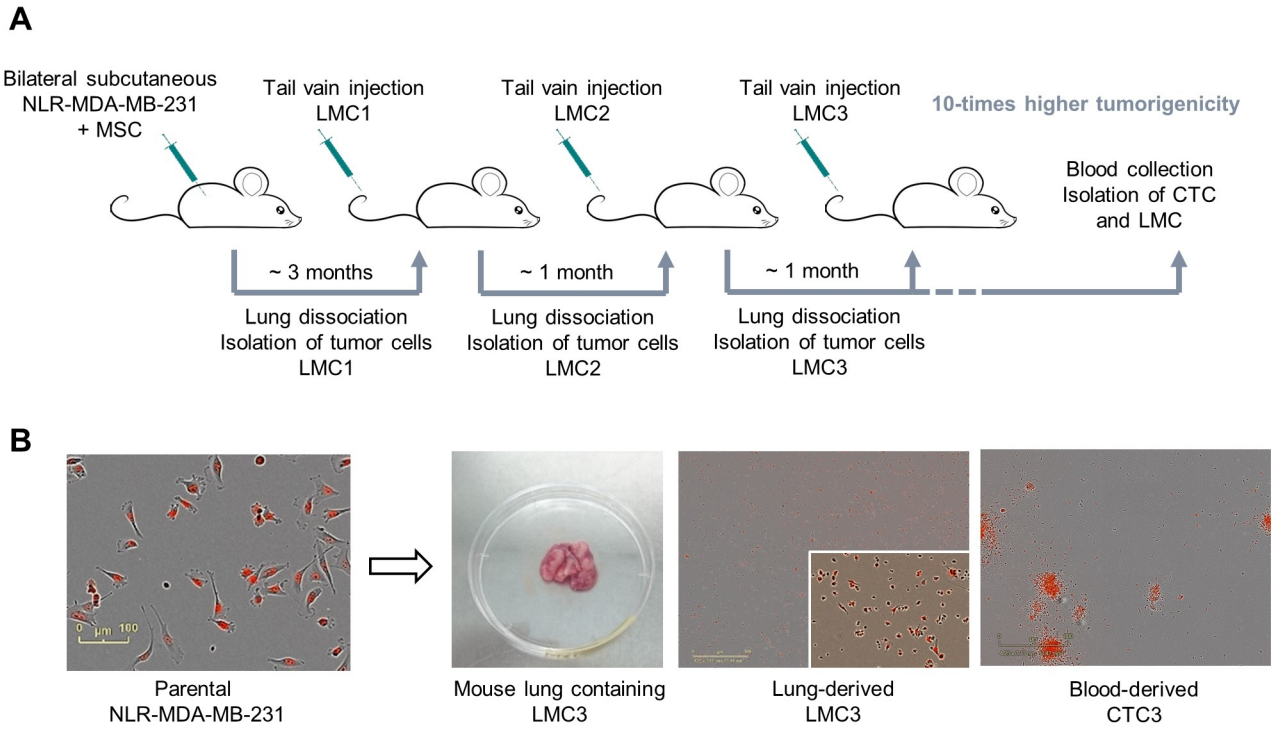

Figure 1. Experimental design of the study. A) Schematic representation of the experimental design of aggressive cell line derivation B) Example photographs of the parental cell line, mouse lung used for cell isolation, lung-derived and blood-derived cancer cells.

the variant in the given selection round, thus the representative data are shown.

Characterization of LMC3 and CTC3 variants *in vitro*. Herein, we compared the basic characteristics of LMC3 and CTC3 *in vitro*. Basic cell morphology was compared using IncuCyte ZOOM™ kinetic imaging system (Figure 2A). For deeper morphology evaluation, actin filaments (F-actin) were stained with a green fluorescent antibody (Figure 2B). We did not detect any significant changes in cytoskeletal actin filaments in derived cells. The proliferation of these cells was similar to the parental cell line NLR-MDA (Figure 2C). Moreover, the cells were tested for chemosensitivity using 5-fluorouracil (5-FU), cyclophosphamide (CPX), paclitaxel (PTX), and cisplatin (CisPt). No significant changes were observed except for sensitivity to doxorubicin (DOX), both variants showed significantly higher resistance to this compound (Figure 2D).

Migration capacity was tested in a standard wound healing assay (Figure 3). Relative wound density was determined by counting wound confluence percentage (Figure 3A). Here, we tested more parallel-derived variants (LMC3/1 = mouse 1, LMC3/2 = mouse 2, etc.) to demonstrate their higher migration capacity in comparison to the parental NLR-MDA cell line *in vitro*. In the case of CTC3/2, we cultured cells on two different Petri dishes (CTC3/2a and CTC3/2b) to compare possible characteristic's alteration caused by passaging but the migration potential remains the same. Images taken 24 hours after wounding were selected as representatives (Figure 3B).

To analyze metastatic cell lines on the molecular level, we used The Human Tumor Metastasis RT² Profiler™ PCR Array to analyze 84 genes associated with the metastatic process to compare LMC3 cells with parental NLR-MDA line. Although the derived line gained high metastatic potential, only 5 out of 84 tested genes had changed expression (cut off 3). We observed upregulation of gene expression of *MMP9* and downregulation of *CDH11, CST7, CXCR4,* and *TNFSF10* (Figure 4).

As previously observed, metastatic isogenic cell line variants differed substantially in the expression of the

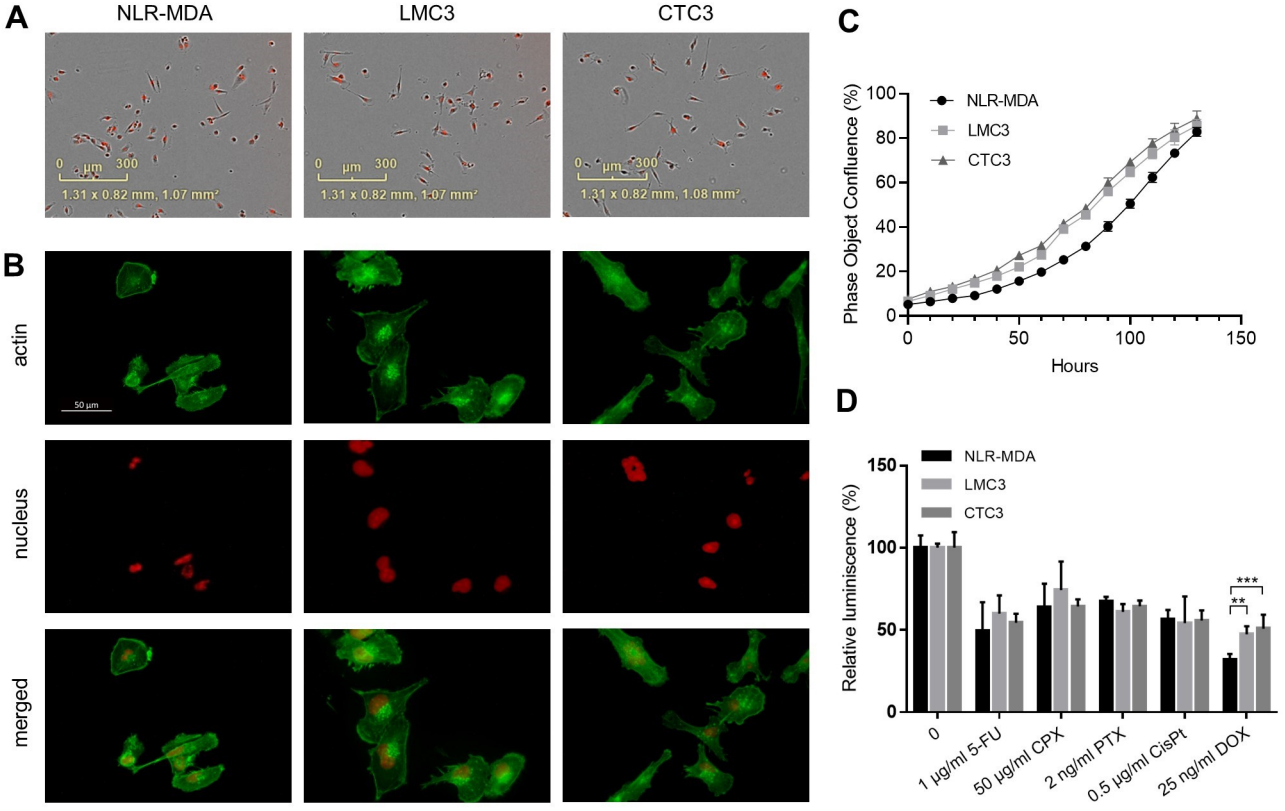

Figure 2. Functional changes in metastatic cancer cell lines A) Phenotype of breast cancer cell lines were documented using bright field and red fluorescence by the IncuCyte ZOOM™ kinetic imaging system and B) actin fluorescence staining (actin-green, nucleus-red, due to the permanent mKate staining) was documented by Zeiss Axiolab 5 FL (magnification ×40). The morphology of parental and derived cells did not differ. C) 7-day proliferation curve showing slightly faster proliferation of lung- (LMC3) and blood- (CTC3) derived cancer cells compared to parental NLR-MDA, although the effect is not significant. D) Luminometric measurement of ATP level after 5-day treatment with 5-FU, CPX, PTX, and CisPt did not show any significant differences in chemosensitivity between tested cell lines. We observed significantly higher resistance to DOX in LMC3 (p=0.0014) and in CTC3 (p=0.0003). Statistically significant results are highlighted with asterisks at *p<0.05, **p<0.01, ***p<0.001.

adhesion molecules and the extracellular matrix composition [16]. Based on these data, we used The Human Extracellular Matrix and Adhesion Molecules RT² Profiler™ PCR Array covering 84 different genes associated with extracellular matrix and adhesion molecules for CTC3 cell line analysis. We identified 5 upregulated genes – *COL6A1, COL6A2, MMP9, SPARC, SSP* – and 11 downregulated – *ADAMTS1, COL12A1, COL15A1, COL8A1, ECM1, FN1, ICAM1, ITGB5, MMP11, THBS1,* and *THBS2* (cut off 3, Figure 5).

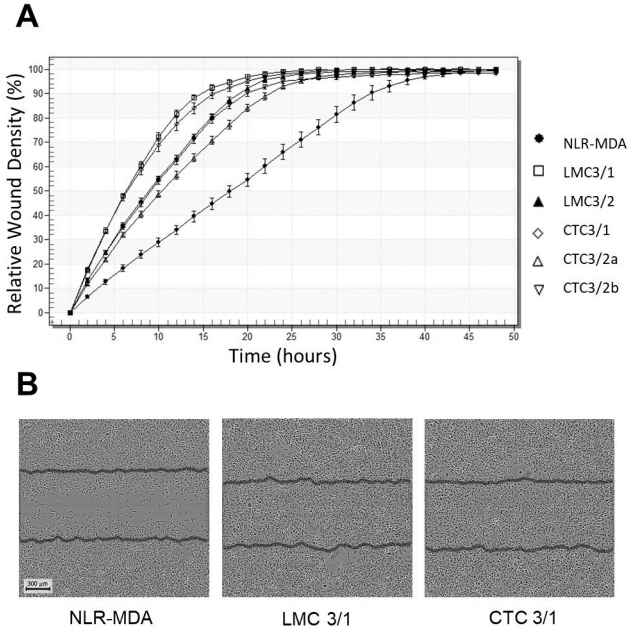

Figure 3. Increased migration potential in the lung- and blood-derived cancer cells *in vitro*. A) Migration potential analysis based on relative wound density showed higher migration of all lung- (LMC3/x) and blood- (CTC3/x) derived cancer cells in comparison with the parental cell line (NLR-MDA). More than one isolate was used to declare a higher metastatic potential. B) Example pictures of NLR-MDA, LMC3, and CTC3 cell migration 24 h after scratch demonstrating increased migration capacity of IV-derived cells.

Characterization of LMC3 and CTC3 variants *in vivo*. To evaluate the tumorigenicity of LMC3 and CTC3 cell lines *in vivo*, immune-compromised female SCID/Beige mice were bilaterally subcutaneously injected with parental, lung- or blood-derived cells. We observed faster tumor growth in mice injected with metastatic LMC3 and CTC3 (Figure 6A). Tumor volumes in mice injected with both derived cell lines were significantly higher than in the case of the parental line before the termination of the experiment. Final average tumor volumes in mice injected with the parental NLR-MDA cells were 75.76 mm^3 (+/– 41.54), in the group injected with LMC3 were 351.47 mm^3 (+/– 255.01), and in the group injected with CTC3 were 407.68 mm^3 (+/– 179.49; Figure 6B). Average tumor weight in the NLR-MDA group was 21 mg (+/– 19.06), in the LMC3 group 122 mg (+/– 88.79), and in the CTC3 group 159.83 mg (+/– 75.68; Figure 6C). All these results showed significant differences and increased tumorigenicity of novel cell variants.

To assess the metastatic potential of derived cells, parental NLR-MDA and metastatic LMC3 and CTC3 cell lines were intravenously injected into the tail vein of female NSG mice, because these animals have more severe immunodeficiency. Blood and bone marrow were checked for the presence of viable red fluorescent cells (Table 1). We found cancer cells in the blood of all animals but with a higher number in mice injected with derived cell lines compared to parental NLR-MDA. No cancer cells were detected in the bone marrow of mice injected with parental cell line. Viable tumor cells in bone marrow were detected only in one mouse injected with a lung-derived cell line and in all six out of six mice injected with blood-derived cancer cells within 3 weeks after inoculation. Importantly, our CTC3 model cells produce detectable metastases in the lungs, bone marrow, and a detectable amount of viable CTC in the blood within 3 weeks, which makes them unique candidate to test the effect of therapeutics of gene alteration on the tumor burden *in vivo*.

Histological staining of the lungs, livers, and brains with hematoxylin and eosin (Table 1) showed metastases in 11

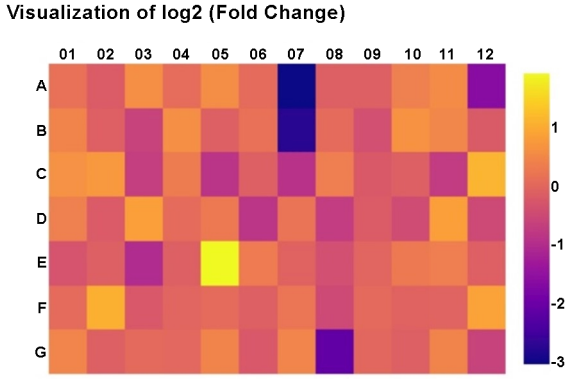

Position	Gene	Fold Regulation
E05	MMP9	3.82
A07	CDH11	-8.21
A12	CST7	-3.09
B07	CXCR4	-6.86
G08	TNFSF10	-4.37

Figure 4. Altered expression profile of metastasis-related genes in LMC3 RT² Profiler™ PCR Array Human Tumor Metastasis was used to assess gene expression changes in lung-derived LMC3 cell line. Only five out of 84 metastasis-related genes (shown in the table with accurate fold change value) showed higher than 3-fold up- or down- regulation compared to the parental NLR-MDA cell line.

out of 12 analyzed lung samples, while only small isolated groups of metastatic cancer cells were found in mice injected with the parental cells (3 out of 3) and mice isolated with lung-derived cells (2 out of 3). Massive metastatic carcinoma was identified in one mouse with lung-derived cells and in all mice injected with blood-derived cells (6 out of 6). In one of these cases, we were able to identify metastatic spread also in the liver. No animals exhibited metastases in the brain according to this staining. The percentage of the lung area covered by cancer cells in each mouse is shown in Table 2. Representative pictures of lungs stained with HE from each group of injected mice are shown in Figure 6D. Lungs were additionally immunohistochemically stained with Ck7, Ck20, and Ki-67 – percentage results confirming the highest metastatic potential of blood-derived cancer cells are shown in Table 2 and representative pictures in Figure 6E. Ck20 was negative in all tested samples.

Discussion

The molecular mechanism of the metastatic processes is not fully understood yet and needs to be further elucidated. To be able to study these mechanisms, laboratory metastatic models need to be available. Here, we derived highly aggressive metastatic and CTC-producing cell lines for rapid and cost-efficient functional testing.

TNBC treatment involves mainly conventional cytotoxic systemic chemotherapy. Therefore, there is a great clinical need to study CTC dissemination and metastatic outbreak. In general, for exploring the molecular mechanisms of cancer biology as well as developing better clinical models to test novel therapeutic strategies, mouse models provide critical insights into cancer research. Indeed, there are many laboratory models for investigating breast cancer (reviewed in Roarty and Echeverria [12]). There was a great trend to use orthotopic metastasis mice models, which, unfortunately, require months to metastasize to distant organs. On the other hand, intravenous (IV) injection of cancer cells directly into the mouse bloodstream mimics the advanced stages of metastatic cascade and takes only a few weeks to develop metastasis. Early in 2013, Rashid et al. published the genomic profile comparisons of lung metastases derived from orthotopic and IV breast cancer cell injection [17]. They did not find significant differences between them and thus, lung metastases formed after IV injection are considered as a relevant breast cancer metastatic model.

Fidler with his colleague found out that only subpopulations of cancer cells possess metastatic abilities, and these could be clonally selected to derive lines with enhanced metastatic seeding to a particular organ [18]. There is an estimation that in animal models only 0.02% of cancer cells develop metastatic abilities [19]. We were able to isolate metastatic breast cancer cells from mice lungs after the first co-injection with MSC. The selection was based on the red fluorescence and puromycin resistance of the injected fluorescently labeled MDA-MB-231 cells (mentioned above as NLR-MDA). LMC3 metastatic cells were derived by repeated injection of tumor cells into the tail vein of immunodeficient mice and subsequent selection of metastatic cells from lung metastases. It is well known, that in the blood of stage IV breast cancer patients CTC can be frequently found [20].

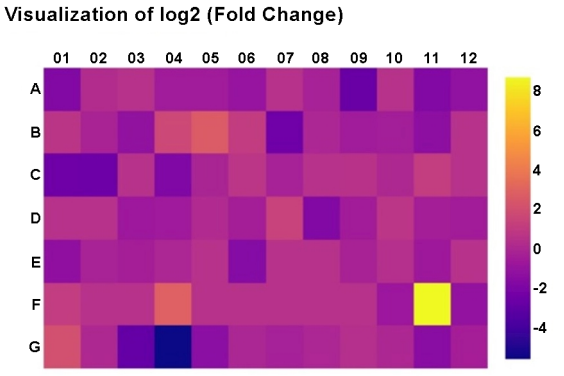

Position	Gene	Fold Regulation
B04	COL6A1	3.08
B05	COL6A2	6.03
F04	MMP9	7.37
F11	SPARC	419.21
G01	SPP1	4.17
A01	ADAMTS1	-3.50
A09	COL12A1	-6.67
A11	COL15A1	-3.48
B07	COL8A1	-5.69
C01	ECM1	-5.77
C02	FN1	-6.01
C04	ICAM1	-3.73
D08	ITGB5	-3.48
E06	MMP11	-3.27
G03	THBS1	-7.67
G04	THBS2	-48.45

Figure 5. Altered expression profile of ECM-related genes in CTC3 RT² Profiler™ PCR Array Human Extracellular matrix and adhesion molecules were used to assess gene expression changes in blood-derived CTC3 cell line. Sixteen out of 84 metastasis-related genes (shown in the table with accurate fold change value) showed higher than 3-fold up- or down-regulation compared to the parental NLR -MDA cell line.

Table 1. Detection of breast cancer cells in the blood, bone marrow, lung, brain, and liver of mice injected with parental NLR-MDA, lung-derived LMC3, and blood-derived CTC3 cells.

	NLR-MDA			LMC3			CTC3					
	mouse 1	mouse 2	mouse 3	mouse 1	mouse 2	mouse 3	mouse 1	mouse 2	mouse 3	mouse 4	mouse 5	mouse 6
Blood	+	+	+	+	+	+++	+++	++	+	++	++	+
Bone marrow	–	–	–	–	–	+	++	+	++	+++	++	+++
Lung	+	+	+	+	–	+++	+++	+++	+	+++	+++	+++
Brain	–	–	–	–	–	–	–	–	–	–	–	–
Liver	–	–	–	–	–	–	–	–	–	–	+	–

Notes: semi-quantitative evaluation of cancer cells occurrence: – no cancer cells present; +, ++, +++ apparent amount of cancer cells (from the lowest to the highest)

Table 2. Results of H&E and IHC staining of lung tissues.

	H&E staining (%)		IHC staining (%)	
	tumor tissue	healthy lung tissue	Ck7	Ki-67
NLR-MDA mouse 1	5	95	70	70
NLR-MDA mouse 2	5	95	60	60
NLR-MDA mouse 3	5	95	70	50
LMC3 mouse 1	5	95	50	50
LMC3 mouse 2	0	100	70	60
LMC 3 mouse 3	70	30	10	60
CTC3 mouse 1	60	40	60	70
CTC3 mouse 2	40	60	40	50
CTC3 mouse 3	10	90	20	60
CTC3 mouse 4	70	30	20	70
CTC3 mouse 5	70	30	0	90
CTC3 mouse 6	70	30	40	50

Therefore, we also processed blood in addition to the lung to isolate CTC and established a CTC3 line without any special isolation technique (CTC isolation techniques are reviewed in Sharma et al. [21]). Even though we injected cancer cells directly into the bloodstream, it is very unlikely that those cells were able to survive in the blood for such a long time. According to Meng et al., CTC have a very short survival time in the bloodstream, estimated in the range from 1 to 3 hours [22]. Therefore, we assume that the injected cells first needed to colonize tissues or organs in the mice shortly after the injections, and cells found in the blood were the result of the advanced metastatic process.

The cell line models were tested for various functional and molecular characteristics. Under the phase-contrast microscope, there were no shape differences between the parental and lung- or blood-derived cells. We did not observe any major changes in actin filaments either. Metastatic cancer cells for many different cancers are known to have altered cytoskeletal properties – usually more deformable and contractile. There are cases, where metastatic cancer cells have more mesenchymal cell shape than parental ones. On the contrary, some metastatic cells have a rounder shape than their non-metastatic versions [23]. In our case, parental NLR-MDA cells are metastatic *per se*, therefore their even more metastatic derivates can easily keep their original shape.

We did not observe any significant differences in cell proliferation or sensitivity to the panel of 4 different chemotherapeutics, namely 5-FU, CPX, PTX, and CisPt. However, lung- and blood-derived cells were significantly more resistant to DOX. As mentioned before, systematic chemotherapy is the most common treatment option for TNBC patients. Although DOX is currently considered to be one of the most effective chemotherapeutic agents in breast cancer treatment, its resistance leads to an unsuccessful outcome in many patients. Although the mechanisms of DOX resistance remain unclear, it is accepted that its development is a multifactorial phenomenon. Investigations into the factors triggering the observed DOX resistance revealed that a decrease in cell-to-ECM adhesion played a pivotal role [24], which we observed in decreased expression of different types of collagens, integrins, and various adhesion molecules. Also, an increased expression of *MMP9* was correlated with the advancement of resistance to higher concentrations of DOX [25], which is also in correlation with our results.

We observed the higher migration capacity of LMC3 and CTC3 compared to the parental cell line *in vitro*, which was in accordance with our *in vivo* data and also expected in highly metastatic cell lines.

We also examined the expression of genes associated with signaling pathways related to the metastasis in our metastatic lung-derived cell line LMC3. An RT-PCR array of 84 different genes identified the largest expression differences in 5 genes. The only upregulated gene was *MMP9*, which has several important roles in processes such as extracellular matrix (ECM) remodeling, metastasis, and angiogenesis [26]. In breast cancer, Owyong and colleagues have shown that MMP9 is a crucial component of the metastatic niche and promotes CTC to colonize the lungs [27]. We observed the downregulation of *CDH11*, *CST7*, *CXCR4*, and *TNFSF10* genes. Cadherin-11 (CDH11) has been for a long time recognized as a protein expressed in invasive breast cancer. There are cancer cells that lost CDH11 – they are either poorly invasive with a rounded phenotype, or highly invasive with a mesenchymal phenotype [28]. Later, an alternatively-spliced variant of CDH11 was identified in breast cancer cell lines to promote invasiveness [29]. Nevertheless, there are many scientific papers that recognize the higher expression of *CDH11* in invasive cancers. Therefore, in our

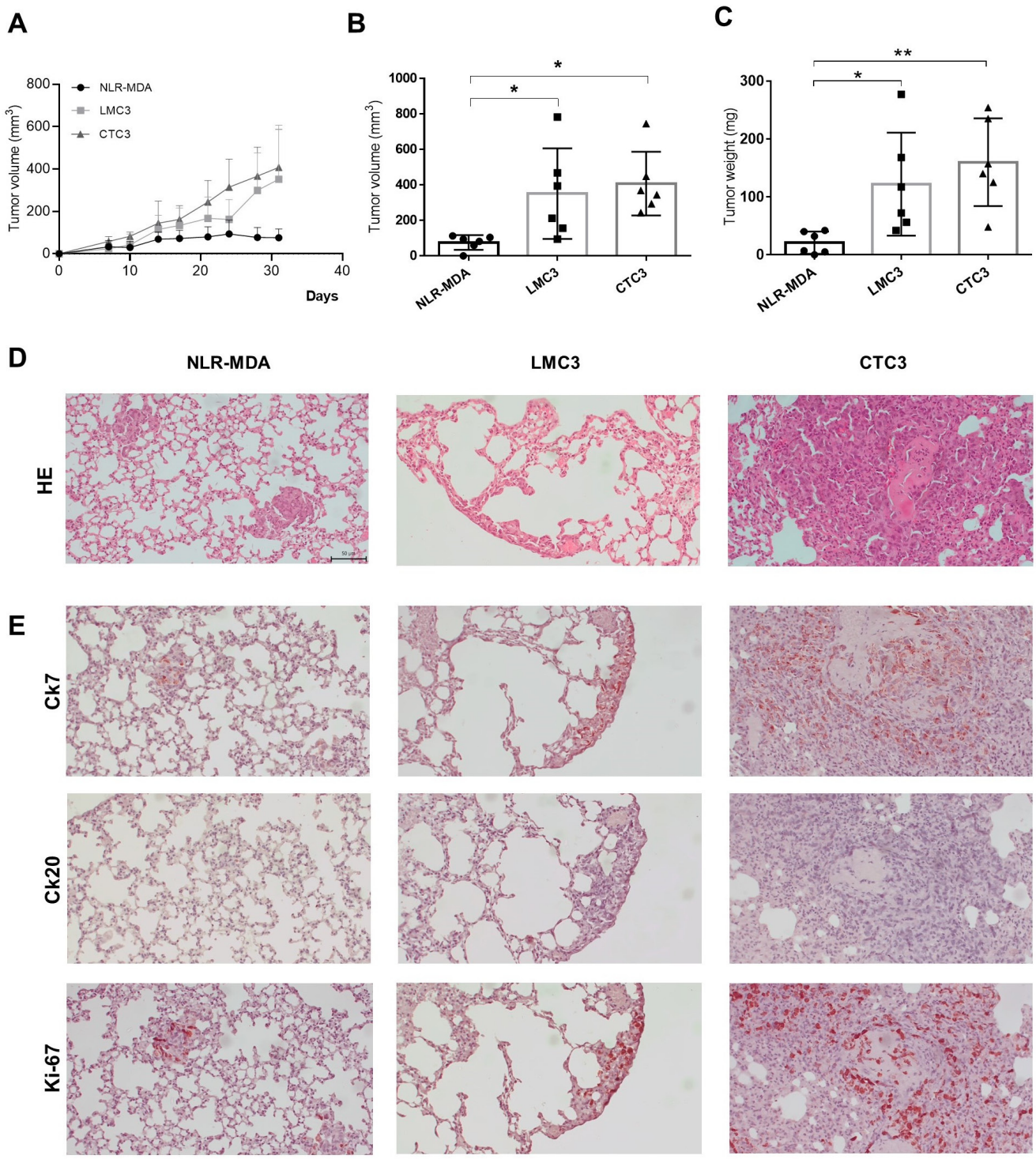

Figure 6. Increased tumorigenic and metastatic effects of LMC3 and CTC3 *in vivo*. A) Tumor volume evaluation in time – we observed faster tumor growth in both, LMC3 and CTC3, cell lines compared to the parental NLR-MDA line. Tumor volumes were calculated according to the formula volume = (length × width^2)/2. B) Tumor volumes from the last measurement before the ending of the experiment were statistically evaluated (lung-derived LMC3 cell line, p=0.0346; blood/derived CTC3, p=0.0119) C) Tumor weights measured after the experiment termination. We observed significantly higher tumor mass in both tested groups (lung-derived LMC3 cell line, p=0.0394; blood/derived CTC3, p=0.0058). D) Representative pictures of hematoxylin-eosin (H&E) staining and E) immunohistochemically Ck7, Ck20, and Ki-67 staining of mice lungs intravenously injected with parental NLR-MDA, lung-derived LMC3, and blood-derived CTC3 cells showed the higher metastatic potential of blood-derived cell line compared to the parental and lung-derived cells (magnification 20×). Statistically significant results are highlighted with asterisks at *p<0.05, **p<0.01.

case, downregulation of *CDH11* could either mean high invasiveness because of the mesenchymal phenotype of the cells or may be misleading as there are many splice variants that induce invasiveness and the expression array does not recognize some of these variants (out of which some may be still overexpressed). The rest of the genes that we found downregulated were often found upregulated during the metastatic process in other studies. Although it may sound a little controversial, one needs to be careful when making generalized conclusions. For example, *CXCR4* is known to be highly expressed in MDA-MB-231 cells [30]. Therefore, *CXCR4* downregulation in LMC3 could still mean that the CXCR4 receptor is highly upregulated in comparison to the healthy cells or that CXCR4 signaling pathways are not the ones that make these metastatic cells so aggressive.

To analyze CTC3, we used a panel of 84 genes related to the ECM and adhesion molecules. As mentioned above, cancer cells need to undergo EMT, which involves rearrangement in the ECM and changes in their adhesion, to enter the bloodstream and metastasized into distant organs. Change of expression above the predetermined threshold was observed in sixteen of the tested genes, and the change in two of them (*SPARC* and *THBS2*) greatly exceeded the others. The secreted protein acidic and rich in cysteine (SPARC) is a matricellular glycoprotein that has been extensively associated with breast cancer aggressiveness although the underlying mechanisms are still not completely clear. It is frequently overexpressed in breast tumors with the highest expression rates in TNBC [31]. Even in primary breast tumors, a high level of SPARC protein is associated with worse disease-free survival and overall survival than patients with low SPARC level [32]. Therefore, increased *SPARC* expression may serve as an indicator of greater aggressiveness, and as a prognostic factor for TNBC. In the study of Ma et al., increased expression of SPARC correlated with a low rate of bone metastasis [33]. In total, 60–70% of patients with metastatic breast cancer have bone metastases [34]. Even though TNBC usually does not metastasize into the bone marrow [12], and even despite high gene expression of *SPARC*, we were able to detect bone marrow metastases in mice injected with lung-derived LMC3 and blood-derived CTC3 cells.

The role of thrombospondin 2 (*THBS2*, TSP-2) in breast cancer remains controversial. Firstly, TSP-2 acts as an important naturally occurring angiogenesis inhibitor. Naturally, tumor growth depends on the angiogenic process (reviewed in Koch [35]). In the study of Lin et al., THBS2 was indicated to inhibit the proliferation, migration, and invasion abilities of TNBC cells *in vitro* [36]. Therefore, our cancer cell lines increase their proliferation rate, tumor growth, and metastatic spread by downregulating the *THBS2* expression. On the other, there are few studies (mostly newly submitted preprints) that showed higher expression of *THBS2* in breast cancer tissue compared to healthy tissue. The survival analysis published by Weng et al. indicated that increased THBS2 expression levels were associated with poor survival rates in breast cancer [37]. One way or another, different proteins could have different roles in different processes. In our case, it is probably the inhibition role of THBS2 in angiogenesis.

In summary, here we describe the molecular and biological comparison of the newly derived isogenic variants of the TNBC cell line MDA-MB-231 that enlarge the pool of established cell lines valuable for rapid and cost-efficient functional testing of novel interventions to block dissemination and appearance of viable CTC in the blood as well as preventive strategies to limit metastatic outgrowth in the lungs and bone marrow.

Acknowledgments: We would like to thank Ms. L. Rojikova for assistance with *in vivo* experiments and Dr. M. Bohac for providing adipose tissue used for MSC isolation. This research was funded by the Slovak Research and Development Agency under contracts APVV 16-0010 and 16-0178; and Scientific Grant Agency (VEGA) under contracts No. 2/0138/20 and 2/0067/22. Also, thanks to the support of the Operational Programme Integrated Infrastructure for the project: Integrative strategy in development of personalized medicine of selected malignant tumors and its impact on quality of life, IMTS: 313011V446, co-financed by the European Regional Development Fund.

References

[1] SUNG H, FERLAY J, SIEGEL RL, LAVERSANNE M, SOERJOMATARAM I et al. Global Cancer Statistics 2020: GLOBOCAN Estimates of Incidence and Mortality Worldwide for 36 Cancers in 185 Countries. CA Cancer J Clin 2021; 71: 209–249. https://doi.org/10.3322/caac.21660

[2] BERMAN AT, THUKRAL AD, HWANG WT, SOLIN LJ, VAPIWALA N. Incidence and patterns of distant metastases for patients with early-stage breast cancer after breast conservation treatment. Clin Breast Cancer 2013; 13: 88–94. https://doi.org/10.1016/j.clbc.2012.11.001

[3] GANESH K, MASSAGUÉ J. Targeting metastatic cancer. Nat Med 2021; 27: 34–44. https://doi.org/10.1038/s41591-020-01195-4

[4] VAN ZIJL F, KRUPITZA G, MIKULITS W. Initial steps of metastasis: cell invasion and endothelial transmigration. Mutat Res 2011; 728: 23–34. https://doi.org/10.1016/j.mrrev.2011.05.002

[5] GARMPIS N, DAMASKOS C, ANGELOU A, GARMPI A, GEORGAKOPOULOU VE et al. Animal Models for the Calculation of Circulating Tumor Cells for Experimental Demonstration. Anticancer Res 2020; 40: 6599–6607. https://doi.org/10.21873/anticanres.14684

[6] MORALES M, ARENAS EJ, UROSEVIC J, GUIU M, FERNÁNDEZ E et al. RARRES3 suppresses breast cancer lung metastasis by regulating adhesion and differentiation. EMBO Mol Med 2014; 6: 865–881. https://doi.org/10.15252/emmm.201303675

[7] ZHANG C, LOWERY FJ, YU D. Intracarotid Cancer Cell Injection to Produce Mouse Models of Brain Metastasis. J Vis Exp 2017; 120: 55085. https://doi.org/10.3791/55085

[8] YU C, WANG H, MUSCARELLA A, GOLDSTEIN A, ZENG HC et al. Intra-iliac Artery Injection for Efficient and Selective Modeling of Microscopic Bone Metastasis. J Vis Exp 2016; 115: 53982. https://doi.org/10.3791/53982
[9] ZHOU H, ZHAO D. Ultrasound imaging-guided intracardiac injection to develop a mouse model of breast cancer brain metastases followed by longitudinal MRI. J Vis Exp 2014; 85: 51146. https://doi.org/10.3791/51146
[10] MINN AJ, KANG Y, SERGANOVA I, GUPTA GP, GIRI DD et al. Distinct organ-specific metastatic potential of individual breast cancer cells and primary tumors. J Clin Invest 2005; 115: 44–55. https://doi.org/10.1172/JCI22320
[11] WULF-GOLDENBERG A, HOFFMANN J, BECKER M, BRZEZICHA B, WALTHER W. Patient-Derived Xenografts from Solid Tumors (PDX) for Models of Metastasis. Methods Mol Biol 2021; 2294: 43–58. https://doi.org/10.1007/978-1-0716-1350-4_4
[12] ROARTY K, ECHEVERRIA GV. Laboratory Models for Investigating Breast Cancer Therapy Resistance and Metastasis. Front Oncol 2021; 11: 645698. https://doi.org/10.3389/fonc.2021.645698
[13] ROWAN BG, GIMBLE JM, SHENG M, ANBALAGAN M, JONES RK et al. Human adipose tissue-derived stromal/stem cells promote migration and early metastasis of triple negative breast cancer xenografts. PLoS One 2014; 9: e89595. https://doi.org/10.1371/journal.pone.0089595
[14] PLAVA J, CIHOVA M, BURIKOVA M, BOHAC M, ADAMKOV M et al. Permanent Pro-Tumorigenic Shift in Adipose Tissue-Derived Mesenchymal Stromal Cells Induced by Breast Malignancy. Cells 2020; 9: 480. https://doi.org/10.3390/cells9020480
[15] KUCEROVA L, ALTANEROVA V, MATUSKOVA M, TYCIAKOVA S, ALTANER C. Adipose tissue-derived human mesenchymal stem cells mediated prodrug cancer gene therapy. Cancer Res 2007; 67: 6304–6313. https://doi.org/10.1158/0008-5472.CAN-06-4024
[16] KUCEROVA L, SKOLEKOVA S, DEMKOVA L, BOHOVIC R, MATUSKOVA M. Long-term efficiency of mesenchymal stromal cell-mediated CD-MSC/5FC therapy in human melanoma xenograft model. Gene Ther 2014; 21: 874–887. https://doi.org/10.1038/gt.2014.66
[17] RASHID OM, NAGAHASHI M, RAMACHANDRAN S, DUMUR CI, SCHAUM JC et al. Is tail vein injection a relevant breast cancer lung metastasis model? J Thorac Dis 2013; 5: 385–392. https://doi.org/10.3978/j.issn.2072-1439.2013.06.17
[18] FIDLER IJ, NICOLSON GL. Organ selectivity for implantation survival and growth of B16 melanoma variant tumor lines. J Natl Cancer Inst 1976; 57: 1199–202. https://doi.org/10.1093/jnci/57.5.1199
[19] CHAMBERS AF, GROOM AC, MACDONALD IC. Dissemination and growth of cancer cells in metastatic sites. Nat Rev Cancer 2002; 2: 563–572. https://doi.org/10.1038/nrc865
[20] BIDARD FC, PEETERS DJ, FEHM T, NOLÉ F, GISBERT-CRIADO R et al. Clinical validity of circulating tumour cells in patients with metastatic breast cancer: a pooled analysis of individual patient data. Lancet Oncol 2014; 15: 406–414. https://doi.org/10.1016/S1470-2045(14)70069-5
[21] SHARMA S, ZHUANG R, LONG M, PAVLOVIC M, KANG Y et al. Circulating tumor cell isolation, culture, and downstream molecular analysis. Biotechnol Adv 2018; 36: 1063–1078. https://doi.org/10.1016/j.biotechadv.2018.03.007
[22] MENG S, TRIPATHY D, FRENKEL EP, SHETE S, NAFTALIS EZ et al. Circulating tumor cells in patients with breast cancer dormancy. Clin Cancer Res 2004; 10: 8152–8162. https://doi.org/10.1158/1078-0432.CCR-04-1110
[23] LYONS SM, ALIZADEH E, MANNHEIMER J, SCHUAMBERG K, CASTLE J et al. Changes in cell shape are correlated with metastatic potential in murine and human osteosarcomas. Biol Open 2016; 5: 289–299. https://doi.org/10.1242/bio.013409
[24] LOVITT CJ, SHELPER TB, AVERY VM. Doxorubicin resistance in breast cancer cells is mediated by extracellular matrix proteins. BMC Cancer 2018; 18: 41. https://doi.org/10.1186/s12885-017-3953-6
[25] PARAMANANTHAM A, JUNG EJ, KIM HJ, JEONG BK, JUNG JM et al. Doxorubicin-Resistant TNBC Cells Exhibit Rapid Growth with Cancer Stem Cell-like Properties and EMT Phenotype, Which Can Be Transferred to Parental Cells through Autocrine Signaling. Int J Mol Sci 2021; 22: 12438. https://doi.org/10.3390/ijms222212438
[26] HUANG H. Matrix Metalloproteinase-9 (MMP-9) as a Cancer Biomarker and MMP-9 Biosensors: Recent Advances. Sensors (Basel) 2018; 18: 3249. https://doi.org/10.3390/s18103249
[27] OWYONG M, CHOU J, VAN DEN BIJGAART RJ, KONG N, EFE G et al. MMP9 modulates the metastatic cascade and immune landscape for breast cancer anti-metastatic therapy. Life Sci Alliance 2019; 2: e201800226. https://doi.org/10.26508/lsa.201800226
[28] PISHVAIAN MJ, FELTES CM, THOMPSON P, BUSSEMAKERS MJ, SCHALKEN JA et al. Cadherin-11 is expressed in invasive breast cancer cell lines. Cancer Res 1999; 59: 947–952.
[29] FELTES CM, KUDO A, BLASCHUK O, BYERS SW. An alternatively spliced cadherin-11 enhances human breast cancer cell invasion. Cancer Res 2002; 62: 6688–6697.
[30] DEWAN MZ, AHMED S, IWASAKI Y, OHBA K, TOI M et al. Stromal cell-derived factor-1 and CXCR4 receptor interaction in tumor growth and metastasis of breast cancer. Biomed Pharmacother 2006; 60: 273–276. https://doi.org/10.1016/j.biopha.2006.06.004
[31] LINDNER JL, LOIBL S, DENKERT C, ATASEVEN B, FASCHING PA et al. Expression of secreted protein acidic and rich in cysteine (SPARC) in breast cancer and response to neoadjuvant chemotherapy. Ann Oncol 2015; 26: 95–100. https://doi.org/10.1093/annonc/mdu487
[32] ZHU A, YUAN P, DU F, HONG R, DING X et al. SPARC overexpression in primary tumors correlates with disease recurrence and overall survival in patients with triple negative breast cancer. Oncotarget 2016; 7: 76628–76634. https://doi.org/10.18632/oncotarget.10532
[33] MA J, GAO S, XIE X, SUN E, ZHANG M et al. SPARC inhibits breast cancer bone metastasis and may be a clinical therapeutic target. Oncol Lett 2017; 14: 5876–5882. https://doi.org/10.3892/ol.2017.6925

[34] SOLOMAYER EF, DIEL IJ, MEYBERG GC, GOLLAN C, BASTERT G. Metastatic breast cancer: clinical course, prognosis and therapy related to the first site of metastasis. Breast Cancer Res Treat 2000; 59: 271–278. https://doi.org/10.1023/a:1006308619659

[35] KOCH M, HUSSEIN F, WOESTE A, GRÜNDKER C, FRONTZEK K et al. CD36-mediated activation of endothelial cell apoptosis by an N-terminal recombinant fragment of thrombospondin-2 inhibits breast cancer growth and metastasis in vivo. Breast Cancer Res Treat 2011; 128: 337–346. https://doi.org/10.1007/s10549-010-1085-7

[36] LIN Y, LIN E, LI Y, CHEN X, CHEN M et al. Thrombospondin 2 is a Functional Predictive and Prognostic Biomarker for Triple-Negative Breast Cancer Patients With Neoadjuvant Chemotherapy. Pathol Oncol Res 2022; 28: 1610559. https://doi.org/10.3389/pore.2022.1610559

[37] WENG TY, WANG CY, HUNG YH, CHEN WC, CHEN YL et al. Differential Expression Pattern of THBS1 and THBS2 in Lung Cancer: Clinical Outcome and a Systematic-Analysis of Microarray Databases. PLoS One 2016; 11: e0161007. https://doi.org/10.1371/journal.pone.0161007